Phase-field modelling of solute trapping during rapid solidification of a Si–As alloy

D. Danilov and B. Nestler

Institute of Applied Research, Karlsruhe University of Applied Sciences, Moltkestrasse 30, 76133 Karlsruhe, Germany

Abstract

The effect of nonequilibrium solute trapping by a growing solid under rapid solidification conditions is studied using a phase-field model. Considering a continuous steady-state concentration profile across the diffuse solid-liquid interface, a new definition of the nonequilibrium partition coefficient in the phase-field context is introduced. This definition leads, in particular for high growth velocities, to a better description of the available experimental data in comparison with other diffuse interface and sharp-interface predictions.

Key words: Rapid solidification; Interface segregation; Bulk diffusion; Interface diffusion; Phase-field models.

1 Introduction

Experimental results for binary alloys show that under nonequilibrium conditions, at high growth velocities, impurity concentration could exceed conventional solid solubility limits given by the equilibrium phase diagram. This effect in rapid solidification has been termed solute trapping and it has been studied extensively with experimental, theoretical and numerical methods.

In the sharp interface approach, a discontinuity in the impurity concentration from c_S (in the solid) to c_L (in the liquid) at the interface is assumed, and a partition coefficient is defined by the ratio

$$\text{(sharp-interface) partition coefficient} = \frac{\text{concentration in solid}}{\text{concentration in liquid}} = \frac{c_S}{c_L}. \quad (1)$$

According to experimental results for doped silicon [1,2,3], the partition coefficient increases from its equilibrium value k_e and approaches unity as the interface velocity increases. In these pulsed laser melting experiments, the values of the partition coefficient are not directly measurable, but they can be determined by theoretically fitting experimental dopant profiles. The experimental

results [2] for Si–As alloys are reproduced in Fig. 1. The same transition from an impurity segregation at low growth velocities to a solute trapping effect in rapid solidification has been numerically modelled by molecular dynamics [4] and Monte Carlo [5] methods.

Diverse analytical sharp interface models [6,7,8,9,10] have been suggested to describe this phenomenon. Aziz proposed a continuous growth model [7,8] giving a velocity dependent partition coefficient of the form

$$\frac{c_S}{c_L} = k_A(V) = \frac{k_e + V/V_D}{1 + V/V_D}, \tag{2}$$

where V is the interface velocity and V_D is a diffusion speed corresponding to the interface. This form of nonequilibrium partition coefficient allows to fit experimental data at low and moderate interface velocities $V < 1$ m/s with $V_D = 0.68$ m/s. In the high-velocity regime at $V \simeq 2$ m/s, the experimental data for the two Si–As alloys in Fig. 1 show a much steeper profile than Eq. (2) proposes. This behaviour is also supported by the results of a comparison of the predictions of Eq. (2) with the molecular dynamics simulations (see Fig. 7 of Ref. [4]).

Jackson *et al.* derived an analytical model [10] for nonequilibrium segregation leading to the partition coefficient

$$\frac{c_S}{c_L} = k_J(V) = k_e^{1/(1+A'V)}, \tag{3}$$

where the constant A' depends on the diffusion coefficient and on the interatomic spacing. For $A' = 2.7$ s/m, this model also fits well experimental data and Monte Carlo simulations up to moderate velocities and exhibits a less steeper profile for rapid solidification conditions. This can be seen in Fig. 1 of the present work and in Fig. 2 of Ref. [5]. It should be noted that the best fits of Eqs. (2) and (3) to the experimental data show almost indistinguishable profiles and therefore the comparison in Section 3 is given only to Eq. (2).

Sobolev proposed an extended version [9] of the formula of Aziz taking into account local nonequilibrium effects in the diffusion field discussed in Ref. [11]. The nonequilibrium partition coefficient reads

$$\frac{c_S}{c_L} = k_S(V) = \begin{cases} \dfrac{k_e(1 - (V/V_D^B)^2) + V/V_D}{1 - (V/V_D^B)^2 + V/V_D}, & V < V_D^B, \\ 1, & V \geqslant V_D^B, \end{cases} \tag{4}$$

where V_D^B is a diffusion speed in the bulk liquid. This additional parameter allows one to fit experimental data in the whole range of the interface velocities (Fig. 1), and predicts the transition to a completely partitionless solidification with $c_S = c_L$ in Si–As at a finite velocity $V_D^B = 2.6$ m/s.

The sharp interface description involves solving diffusion equations in the phases and joining their solutions at a hypothetical moving interface of infinitesimally small thickness. However, a transition interfacial region of finite

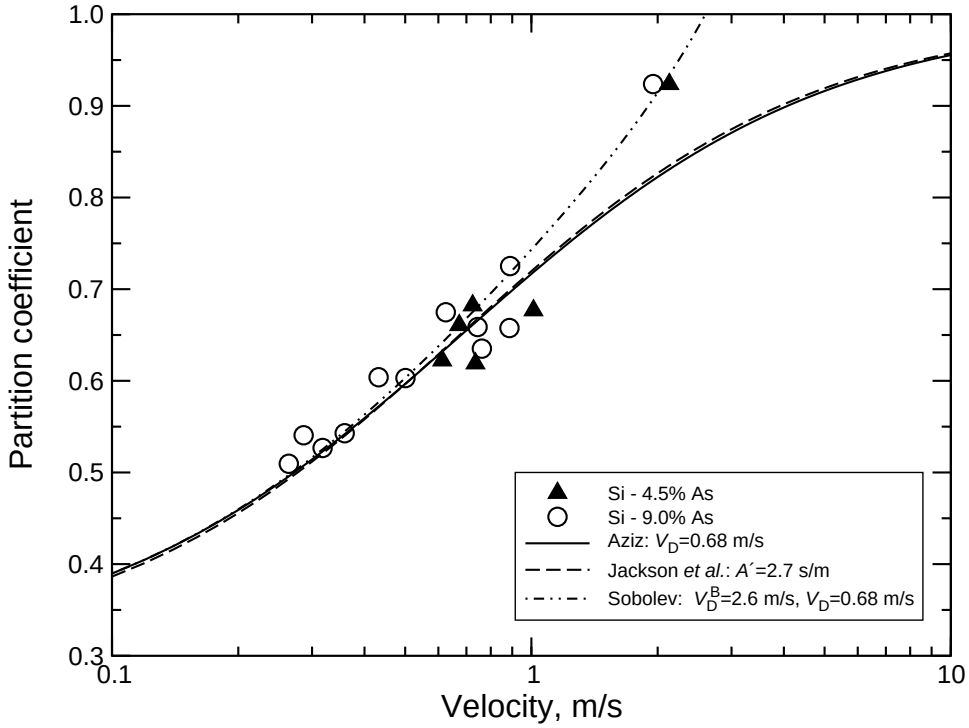

Fig. 1. Experimental data [2] (▲, ○) of the nonequilibrium partition coefficient vs. the interface velocity for two different binary Si–As alloys in comparison with diverse analytical sharp interface models of solute trapping (Eqs. (2)–(4)) assuming an equilibrium partition coefficient of $k_e = 0.3$ [12].

thickness physically always exists between the solid and liquid phases. This fact and the effect of the interaction between the interfacial zone and the diffusion profile in the liquid (with small diffusion length scale comparable to the interface thickness at high growth velocities) are included in the sharp-interface formulation in an implicit way by a separate consideration of the interface and of the bulk processes. During the last two decades, phase-field approaches such as those of Refs. [13,14] have extensively been developed to describe phase transitions. A phase-field model considers in a more realistic way the diffuse character of the interface with a finite thickness and describes the dynamical phenomena in both the bulk phases and the interface region in terms of a single formalism. Much finer scales of the system are resolved taking into account details of the concentration profile in the interfacial region. The concentration profile becomes a continuous function of the coordinate. The specific jump in the concentration at the interface which is typical for a sharp interface formulation disappears and is replaced by a continuous profile with a characteristic maximum near the transition region. Fig. 2 exemplarily illustrates the concentration profiles of sharp interface (dashed line) and diffuse interface (solid line) models. During the solidification of alloys, solute is rejected ahead of the growing solid due to the smaller solubility in the

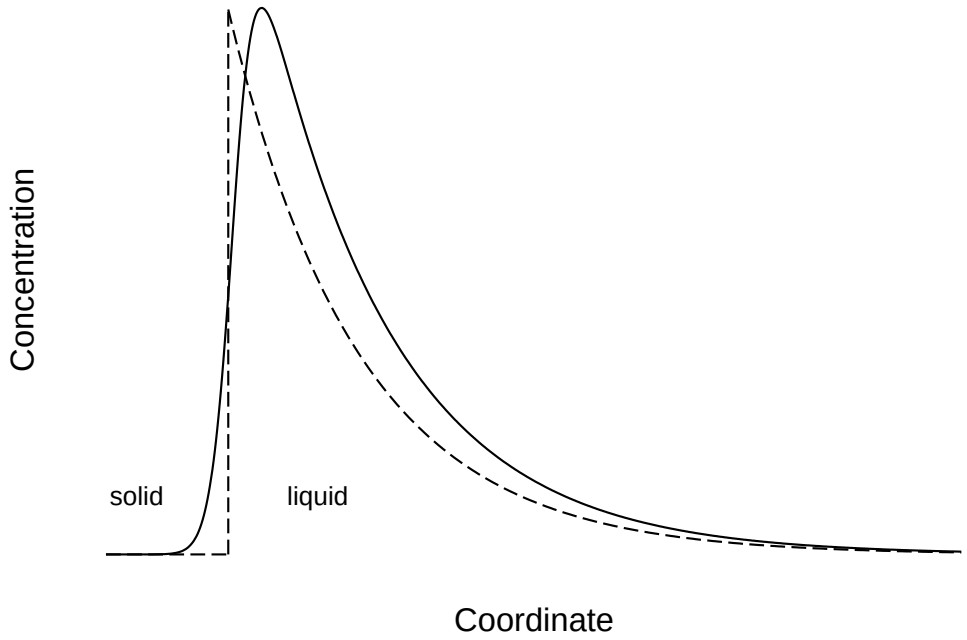

Fig. 2. Discontinuous sharp interface concentration profile (dashed line) and continuous diffuse interface concentration profile (solid line) across a moving solid–liquid interface.

solid phase for partition coefficients $k_e < 1$ (see e.g. Ref. [15]). In steady-state growth, a concentration boundary layer is established as a result of the diffusion of atoms.

In the case of a diffuse interface, there is no possibility to relate a boundary between the solid and liquid phase with a determined coordinate point and to define further the concentration in the phases adjacent to the interface (in analogy to sharp-interface models). Therefore, the definition of the partition coefficient in Eq. (1) is inapplicable in a phase-field approach and needs revision. Wheeler *et al.* [16] and later Ahmad *et al.* [17] considered rapid solidification and solute trapping in terms of a phase-field model and suggested the following definition:

$$\text{(phase-field) partition coefficient} = \frac{\text{far-field concentration}}{\text{maximum of the concentration}}. \qquad (5)$$

The definition in Eq. (5) is valid only for steady-state growth conditions, when the concentration in the bulk solid is equal to the far-field concentration in the liquid. Applied to the parameters of a Ni–Cu alloy, the partition coefficients in Eqs. (2) and (5) exhibit a good agreement in the whole range of interface velocities (see Fig. 2 of Ref. [17]). Using this approach, solute trapping has been further studied in a diffuse interface model by Kim *et al.* [18,19] and with numerical methods by Conti [20]. A rigorous mathematical investigation of the interfacial conditions and of the solute trapping is provided by Glasner [21].

The purpose of this paper is to examine the concentration profiles and corresponding solute trapping effects at a moving planar interface using a thermodynamically consistent phase-field model. We compare the results with available experimental data [2] for a nonequilibrium partition coefficient in Si–As alloy. We focus on the high growth velocity regime, $V > 1$ m/s, because for low and intermediate velocities different models already describe the experimental data with equal success. A definition of the partition coefficient at the diffuse interface is suggested predicting a steeper profile for high growth velocities, $V > 1$ m/s, in accordance with the experimentally measured data of the nonequilibrium partition coefficient.

2 Phase-field model

We use the phase-field formulation for alloy solidification that has recently been proposed in Refs. [22,23] for a general class of multicomponent and multiphase systems. The model is based on an entropy functional and the evolution equations are derived to be consistent with the first (positive local entropy production) and second (conservation equations) laws of thermodynamics. The general case of multiple components is reduced to two phases (solid and liquid) and to a binary alloy with components A (solvent) and B (solute). We apply typical assumptions often made in theories of solidification processes in binary systems: an ideal solution and isothermal approximation. A constant temperature T is considered as a parameter and the free energy density f is postulated in the form

$$f(c_A, c_B, \varphi) = \frac{RT}{v_m}\left(c_A \ln c_A + c_B \ln c_B\right) + \frac{RT}{v_m}\left[c_A \ln\left(\frac{1 + (T_A - T)/m_e}{1 + k_e(T_A - T)/m_e}\right) - c_B \ln k_e\right] h(\varphi), \quad (6)$$

where T_A is the melting point of the pure component A, c_A and c_B are the concentrations of the alloy components given in molar fractions, k_e and m_e are the partition coefficient and the liquidus slope of the equilibrium phase diagram, v_m is the molar volume and R is the gas constant. The phase-field variable φ describes the thermodynamic state of a local volume. The value $\varphi = 1$ corresponds to the solid phase, $\varphi = 0$ corresponds to the liquid and the function $h(\varphi) = \varphi^2(3 - 2\varphi)$ is monotonic in the interval $[0, 1]$ satisfying the conditions $h(0) = 0$ and $h(1) = 1$ in the bulk phases. The form of the free energy density in Eq. (6) leads to an equilibrium phase diagram with straight solidus $T_S = T_A + m_e c_B/k_e$ and liquidus $T_L = T_A + m_e c_B$ lines by a conventional common tangent construction.

Considering a planar solid-liquid interface, we write the evolution equations of the phase-field model for isotropic kinetics and isotropic surface energies of the interface. The evolution of the phase-field variable φ is determined by the

partial differential equation

$$\frac{2\varepsilon\gamma}{\nu}\frac{\partial\varphi}{\partial t} = 2\varepsilon\gamma\frac{\partial^2\varphi}{\partial x^2} - \frac{9\gamma}{\varepsilon}\frac{\partial g(\varphi)}{\partial\varphi} - \frac{1}{T}\frac{\partial f}{\partial\varphi}, \tag{7}$$

where $g(\varphi) = \varphi^2(1-\varphi)^2$ is a double well potential, γ is the entropy density of the solid–liquid interface, ν is the interface mobility and the parameter ε determines the thickness of the interfacial zone. The concurrence between the first and the second terms on the right-hand side of Eq. (7) generates the diffuse transition zone between the phases. The last term drives the growth.

The diffusion mass transport of the alloy component B is determined by the nonlinear diffusion equation

$$\frac{\partial c_B}{\partial t} = \frac{\partial}{\partial x}\left(D(\varphi)\frac{\partial c_B}{\partial x}\right) - \Theta\frac{\partial}{\partial x}\left(D(\varphi)c_B(1-c_B)\frac{\partial h}{\partial x}\right), \tag{8}$$

where $D(\varphi) = \varphi D_S + (1-\varphi)D_L$ with constant diffusion coefficients D_S and D_L of component B in the solid and in the liquid phase, respectively. To derive Eq. (8), the constraint condition $c_A + c_B = 1$ has been applied. The quantity Θ denotes the driving force for the redistribution of the alloy components at the solid–liquid interface:

$$\Theta = \ln\left(\frac{1+(T_A-T)/m_e}{1+k_e(T_A-T)/m_e}\right) + \ln(k_e). \tag{9}$$

Growth far from the equilibrium is usually accompanied by a steady-state motion of the interface leading to steady-state concentration profiles. Thus it is useful to consider the velocity V and the solute concentration c_0 in the liquid far from the interface as control parameters whereas the self-consistent temperature and the interfacial concentration will be determined by Eqs. (7) and (8). Looking for a steady-state solution, we adopt a frame of reference

$$z = x - Vt, \tag{10}$$

propagating at a constant velocity V and coincident with the centre of the interfacial zone given by $\varphi = 1/2$ at $z = 0$. Eqs. (7) and (8) read

$$-V\frac{2\varepsilon\gamma}{\nu}\frac{\partial\varphi}{\partial z} = 2\varepsilon\gamma\frac{\partial^2\varphi}{\partial z^2} - \frac{9\gamma}{\varepsilon}\frac{\partial g}{\partial\varphi} - \frac{1}{T}\frac{\partial f}{\partial\varphi}, \tag{11}$$

$$-V\frac{\partial c_B}{\partial z} = \frac{\partial}{\partial z}\left(D(\varphi)\frac{\partial c_B}{\partial z}\right) - \Theta\frac{\partial}{\partial z}\left(D(\varphi)c_B(1-c_B)\frac{\partial h}{\partial z}\right). \tag{12}$$

To investigate the dependence of the concentration profile and the system temperature on the growth velocity, we have computed the numerical solutions

of the nonlinear Eqs. (11) and (12) with associated boundary conditions

$$\begin{aligned} \varphi|_{z\to-\infty} = 1, \quad \varphi|_{z\to+\infty} = 0, \\ \frac{\partial c_B}{\partial z}|_{z\to-\infty} = 0, \quad c_B|_{z\to+\infty} = c_0. \end{aligned} \tag{13}$$

The spatial derivatives have been discretised using finite differences on a uniform grid. A relaxation method is used to obtain the solution of the nonlinear system in Eqs. (11)–(13). Starting from an initial guess ($\varphi^0(z)$, $c^0(z)$, T^0), the successive iterations ($\varphi^n(z)$, $c^n(z)$, T^n) for $n \geqslant 1$ are computed until the convergence criteria $||\varphi^{n+1} - \varphi^n|| < 10^{-9}$ and $||c^{n+1} - c^n|| < 10^{-9} c_0$ are reached, where $||\psi||$ is the L_2-norm of the finite difference representation of a function $\psi(z)$. To ensure smoothness of the numerical solution in the interfacial region, the grid resolution Δx has been chosen from $\Delta x = \frac{1}{20}\varepsilon$ at low velocities to $\Delta x = \frac{1}{80}\varepsilon$ at high velocities.

3 Results

In this section, we consider the application of the model in Eqs. (11) and (12) to solidification of a Si–As alloy. The thermophysical parameters of the alloy are contained in the diffusion equation (diffusion coefficients) and in the entropy contributions: the double well potential, the gradient and the free energy density functions. The values used in the computations are listed in Table 1. The liquidus slope m_e has been estimated from the phase diagram given in Ref. [24]. The value of the interface mobility $\nu = 1.22 \times 10^{-8}$ m^2/s has been adjusted to match the kinetic coefficient $\Delta T/V = 15$ (K·s)/m at high undercoolings ΔT as assumed in Ref. [2]. The work in Refs. [16,17] shows that the magnitude of the solute trapping effect is directly related to the phase-field parameter ε, and a comparison of large-velocity expansions of Eqs. (2) and (5) leads to a relation $V_D \sim D/\varepsilon$ between diffusion speed V_D, diffusion coefficient D, and parameter ε. On this basis, we choose the value of $\varepsilon = 3.5 \times 10^{-9}$ m by fitting the phase-field partition coefficient in Eq. (5) to the sharp interface partition coefficient in Eq. (2) using the value $V_D = 0.68$ m/s provided by comparison with the experimental data (Fig. 1). By this selection of the parameter ε on the physical scale of nanometers no correction terms have been introduced into the model. The inclusion of correction terms such as thin-interface asymptotics in Refs. [25,27] or anti-trapping term in Refs. [26,27] is needed for applications to model dendritic growth and microstructure evolution processes in two and three dimensions at low undercoolings when the interface thickness is some orders of magnitude larger than nanometers. The far-field concentration in the melt has been set to $c_0 = 0.09$ reflecting the alloy composition Si–9 at.% As.

Fig. 3 shows the concentration profiles (solid lines) for three different values of the interface velocity. The concentration profile in the solid phase has a uniform value equal to the far-field concentration c_0 in the liquid. In the inter-

facial region, the concentration increases due to a rejection of solute atoms by the growing solid. In the liquid ahead of the interface, a concentration boundary layer is formed by diffusion transport of the rejected solute atoms into the liquid. With increasing velocity the inhomogeneity of the concentration field reduces. Both the maximum value of the solute concentration as well as the spatial penetration of the concentration profile into the liquid diminish indicating a reduction of solute segregation at the interface as characteristic for the occurrence of solute trapping. The phase-field profile (dashed line) exhibits only a weak dependence on the interface velocity.

To analyse quantitatively the concentration profile, we introduce a characteristic length scale δ describing its thickness by the definition

$$\int_{-\infty}^{+\infty} \Big(c_B(z) - c_0\Big) dz = \Big(c_m - c_0\Big)\delta, \tag{14}$$

where c_m is the maximum of the concentration. From Eq. (14), the corresponding sharp interface steady-state concentration profile [29]

$$\bar{c}(z) = \begin{cases} c_0 + (c_L - c_0)\exp\left(-\dfrac{Vz}{D_L}\right), & z > 0, \\ c_0, & z < 0, \end{cases} \tag{15}$$

leads to the characteristic length scale

$$\delta_{SI} = \frac{D_L}{V}, \tag{16}$$

where the maximum of the concentration c_m corresponds to the interface concentration c_L at the side of the liquid phase. The dependence of the length

Table 1
Physical parameters of Si–9 at.% As alloy used for the phase-field simulations.

Parameter	Value	Reference
T_A	1685 K	[28]
m_e	-400 K	
k_e	0.3	[12]
v_m	12×10^{-6} m^3	
D_L	1.5×10^{-9} m^2/s	[2]
D_S	3×10^{-13} m^2/s	[2]
γ	2.8×10^{-4} J/(K·m^2)	[28]
ν	1.22×10^{-8} m^2/s	
ε	3.5×10^{-9} m	

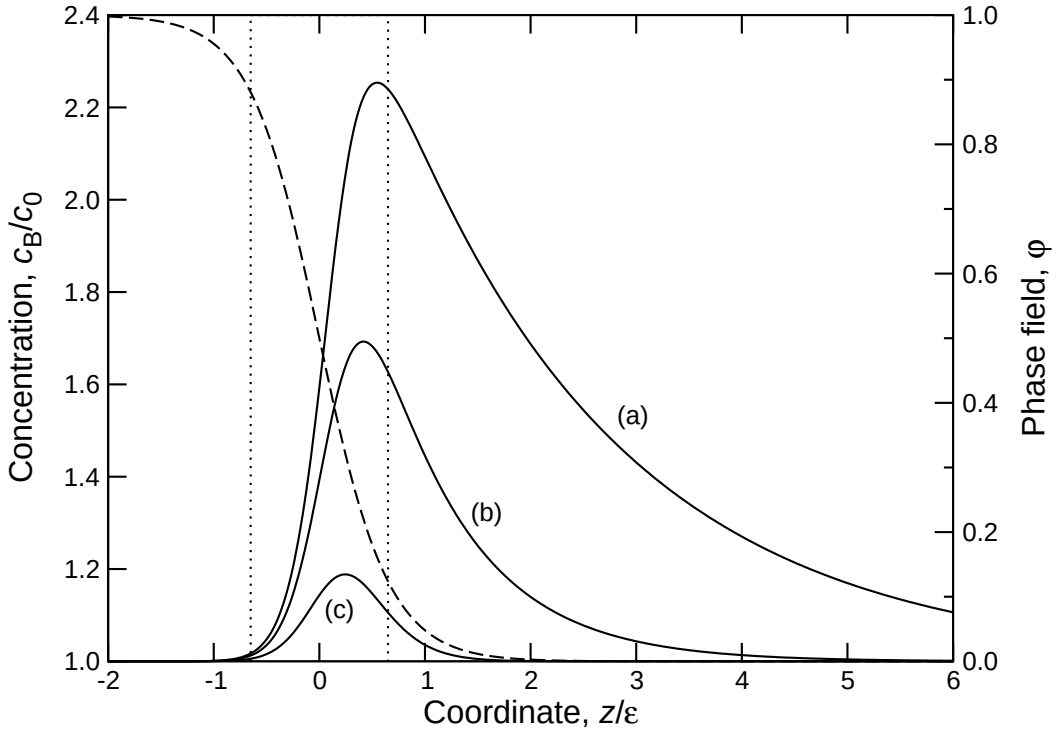

Fig. 3. Steady-state concentration profiles (solid lines) for three different velocities: (a) $V = 0.2$ m/s, (b) $V = 0.5$ m/s, (c) $V = 2$ m/s, and phase-field profile (dashed line) in a reference frame moving in a steady-state manner with the interface.

scales δ and δ_{SI} on the interface velocity V is shown in Fig. 4. At low interface velocities, both δ and δ_{SI} are larger than the interface length scale ε. At high velocities, the thickness δ of the phase-field solution (solid line) approaches a constant value comparable to ε, whereas the thickness δ_{SI} of the sharp interface profile (dashed line) tends to zero. The dotted lines mark the position where the velocity V equals the diffusion speed V_D, i.e. $V = V_D$ and $\delta_{SI} = 0.6\varepsilon$. This position can be considered as a limit for the range of validity of the sharp interface description. At velocities $V > V_D$, the finite thickness of the solid-liquid interface cannot be ignored in the description of the diffusion transport of rejected B-atoms away from the moving interface. The tendency of the length scale δ to become constant as the interface velocity increases is accompanied by a shift of the position of the concentration maximum to the centre of the interfacial zone. Hence, under rapid solidification conditions, the inhomogeneity of the concentration field is completely contained in the diffuse interface region and the concentration field in the bulk liquid tends to the uniform value of the far-field concentration c_0 (Fig. 3 (c)).

Considering Fig. 3, two definitions of the partition coefficient at the diffuse interface are obvious. First, following Wheeler *et al.* [16], the solute concentration in the liquid at the interface is associated with the maximum of the concentration field c_m and the concentration in the solid is assumed to be

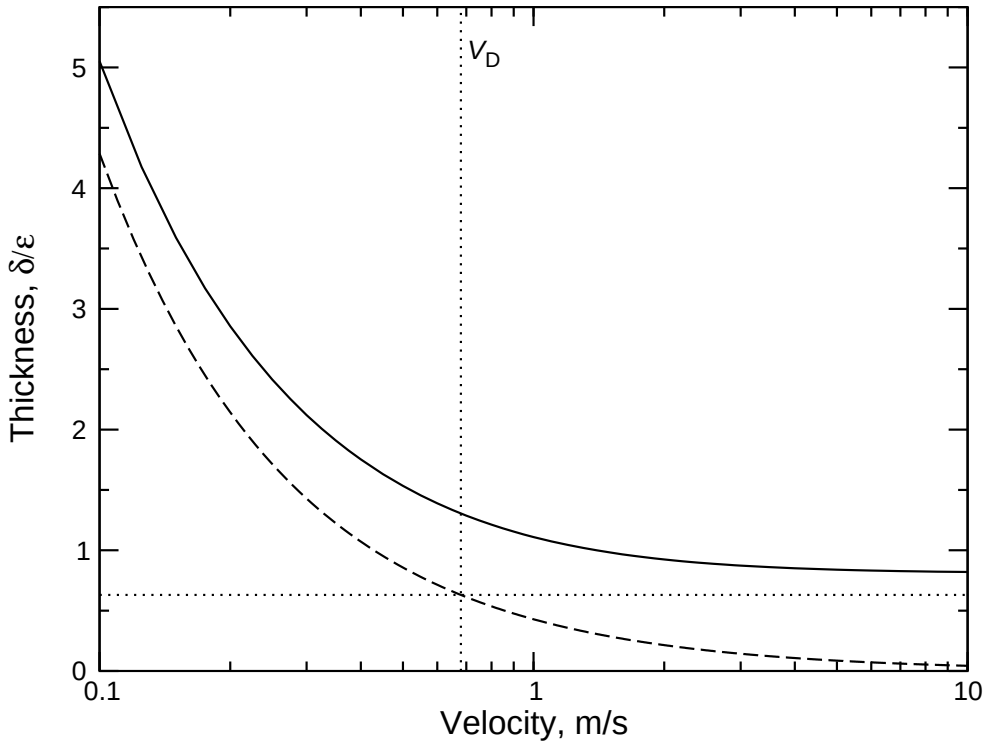

Fig. 4. The dependence of the characteristic length scale δ (solid line) and δ_{SI} (dashed line) on the interface velocity.

equal to c_0. This leads to a partition coefficient k_m that reads

$$k_m = \frac{c_0}{c_m}. \tag{17}$$

Second, in the present work we suggest a definition where the appropriate solid and liquid concentrations for the partition coefficient are determined at positions z_S and z_L in the interior of the diffuse interfacial region leading to the expression

$$k = \frac{c(z_S)}{c(z_L)}. \tag{18}$$

The positions z_S and z_L can be chosen relative to the centre of the interfacial zone in a symmetric way with a best fit criterion to the experimental data.

Fig. 5 displays the different behaviour of the partition coefficients given by Eqs. (2), (4), (17) and (18) as a functions of the interface velocity V. The theoretical models are applied to the alloy system Si–9 at.% As, since experimental data are provided in Ref. [2]. The definition k in Eq. (18) has a steeper profile for high velocities $V > 1$ m/s compared to both the behaviour of k_m in Eq. (17) of the phase-field model for rapid solidification in Ref. [16] and the predictions for k_A in Eq. (2) of the continuous growth model in Refs. [7,8]. For the present data of Si–9 at.% As, the steeper profile is in better agreement with the experimentally measured partition coefficient for $V = 2$ m/s. The

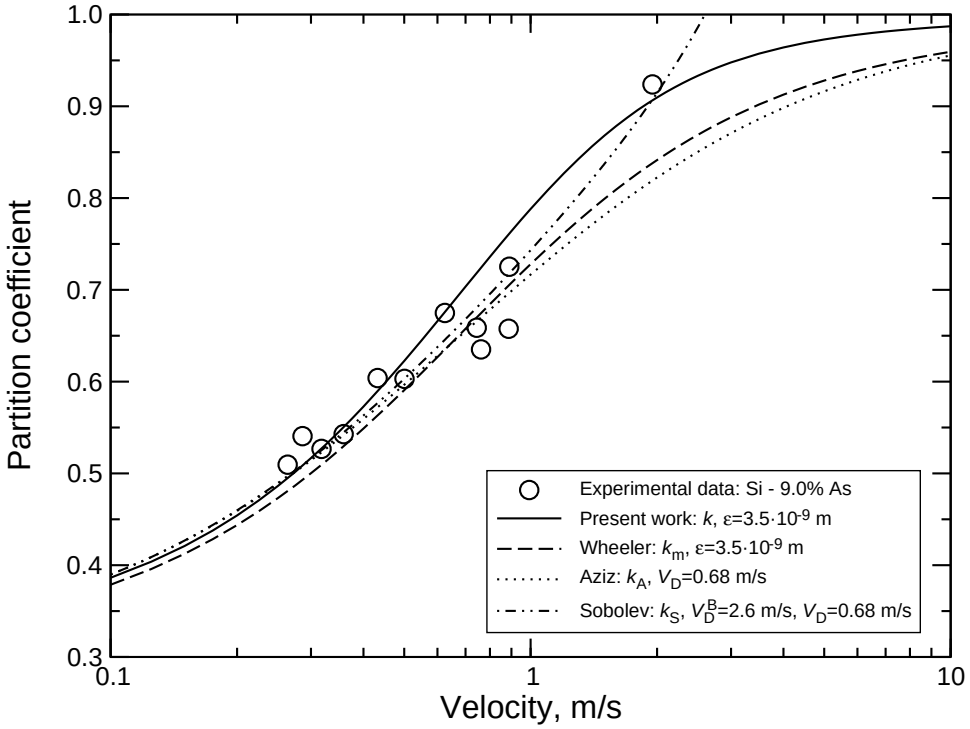

Fig. 5. Different models for the partition coefficient as a function of the interface velocity applied to the alloy system Si–9 at% As and compared with experimental data taken from Ref. [2].

curve of k in Fig. 5 was obtained for the positions $z_S = -0.65\varepsilon$ and $z_L = 0.65\varepsilon$ of the solid and liquid concentrations, respectively. The three approaches for $k(V)$, $k_m(V)$ and $k_A(V)$ show an asymptotic convergence of the partition coefficient to one for $V \to \infty$. The smaller convergence rate for $k_m(V)$ and $k_A(V)$ can exemplarily be illustrated by comparing the values where $1 - k = 1.28 \times 10^{-2}$, $1 - k_m = 4.06 \times 10^{-2}$ and $1 - k_A = 4.46 \times 10^{-2}$ at the velocity $V = 10$ m/s. The value of $1-k_A = 1.28\times10^{-2}$ for the continuous growth model is reached only at a significantly larger velocity $V = 36.4$ m/s. In contrast to the asymptotic convergence of the three approaches for $k(V)$, $k_m(V)$ and $k_A(V)$, the model of Sobolev predicts a sharp transition to $k_S(V) = 1$ at the velocities $V \geqslant V_D$. Thus, the experimental data for rapid solidification can be described by the sharp interface approach in Eq. (4) and by the diffuse interface approach in Eq. (18). However these models predict a qualitatively different character of the transition to establish complete solute trapping.

4 Summary

Considering the continuous concentration profiles at the diffuse solid–liquid interface in Fig. 3, the definition in Eq. (18) of the nonequilibrium partition coefficient in the phase-field description of solute trapping during rapid so-

lidification is proposed. The dependence of the partition coefficient on the interface velocity is compared with other diffuse and sharp interface model predictions. Under the assumption of local equilibrium in the bulk phases, for high interface velocities $V > 1$ m/s, the expression in Eq. (18) gives a steeper profile than previous models, Eqs. (2), (3), (17), and is here in better agreement with the available experimental data for Si–9 at.% As in the range of high growth velocities. Due to a lack of experimental data, a more extended verification of the quantitative character of the transition to complete solute trapping is open: the question to be clarified is whether there exist a sharp transition as predicted by local nonequilibrium solidification model [11] or a smooth continuous transition as predicted by the continuous growth model [7,8] and phase-field models [17].

The presented model of solute trapping can be generalised further by including the effects of local nonequilibrium in the concentration field into the phase-field formulation as described by Galenko [30]. An examination of this effect on the partition coefficient in the diffuse interface approach will be a task for future investigations.

Acknowledgements

This work was supported by the German Research Foundation (DFG) under the priority research program 1120: "Phase transformations in multicomponent melts", Grant No. Ne 822/3-1. The funding is gratefully acknowledged.

References

[1] Aziz MJ, Tsao JY, Thompson MO, Peercy PS, White CW. Phys Rev Lett 1986;56:2489.

[2] Kittl JA, Aziz MJ, Brunco DP, Thompson MO. J Cryst Growth 1995;148:172.

[3] Kittl JA, Sanders PG, Aziz MJ, Brunco DP, Thompson MO. Acta Mater 2000;48:4797.

[4] Celestini F, Debierre JM. Phys Rev B 2000;62:14006.

[5] Beatty KM, Jackson KA. J Cryst Growth 2004;271:495.

[6] Wood RF. Phys Rev B 1982;25:2786.

[7] Aziz MJ. J Appl Phys 1982;53:1158.

[8] Aziz MJ, Kaplan T. Acta Metall 1988;36:2335.

[9] Sobolev SL. Phys Stat Sol (a) 1996;156:293.

[10] Jackson KA, Beatty KM, Gudgel KA. J Cryst Growth 2004;271:481.

[11] Galenko P, Sobolev S. Phys Rev E 1997;55:343.

[12] Reitano R, Smith PM, Aziz MJ. J Appl Phys 1994;76:1518.

[13] Chen LQ. Annu Rev Mater Res 2002;32:113.

[14] Boettinger WJ, Warren JA, Beckermann C, Karma A. Annu Rev Mater Res 2002;32:163.

[15] Kurz W, Fisher DJ. Fundamentals of solidification. TTP, 1998.

[16] Wheeler AA, Boettinger WJ, McFadden GB. Phys Rev E 1993;47:1893.

[17] Ahmad NA, Wheeler AA, Boettinger WJ, McFadden GB. Phys Rev E 1998;58:3436.

[18] Kim SG, Kim WT, Suzuli T. Phys Rev E 1999;60:7186.

[19] Kim WT, Kim SG. Mater Sci and Eng A 2001;304–306:220.

[20] Conti M. Phys Rev E 1997;56:3717.

[21] Glasner K. Physica D 2001;151:253.

[22] Garcke H, Nestler B, Stinner B. SIAM J Appl Math 2004;64:775.

[23] Nestler B, Garcke H, Stinner B. Phys Rev E 2005;71:041609.

[24] Predel B. Phase Equilibria of Binary Alloys. Springer, 2003.

[25] Karma A, Rappel WJ. Phys Rev E 1996;53:R3017.

[26] Karma A. Phys Rev Lett 2001;87:115701.

[27] Echebarria B, Folch R, Karma A, Plapp M. Phys Rev E 2004;70:061604.

[28] Vinet B, Magnusson L, Fredriksson H, Desré PJ. J Colloid and Interface Science 2002;255:363.

[29] Ivantsov GP. Dokl Akad Nauk SSSR 1951;81:179.

[30] Galenko P, Phys Lett A 2001;287:190.